Effects of More Electric Systems on Fuel Tank Thermal Behaviour

Albert S.J. van Heerden (1), David Judt (1), Craig P. Lawson (1), David Bosak (2)
1: Centre for Aeronautics, Cranfield University, College Rd, Bedfordshire, MK 43 0AL, United Kingdom
a.s.van-heerden@cranfield.ac.uk
2: Meggitt PLC, Holbrook Lane, Coventry, CV6 4AA, United Kingdom

Abstract
With the advent of more electric airframe systems and ultra-high bypass ratio turbofan engines, there is growing interest in the associated thermal implications. In this research project, an aircraft level model that is appropriate to enable investigations into novel thermal management solution on future aircraft is developed. In this paper, an investigation into the effects of more electric systems on the thermal behaviour of fuel tanks in civil transport aircraft is presented. Specifically, the influence of the heat generated by conventional and more electric systems on the fuel tank was modelled and simulated. A fuel thermal model was developed, which consists of a tank geometry representation, coupled to a module that calculates remaining mission fuel mass. The systems architectures are represented by connected thermal component models. Standard approaches were then employed to estimate convection and conduction heat transfer coefficients at the tank interfaces. The model solves 1-D transient heat equations, coupling heat transfer and material heat capacity via heat flux balances. The thermal and systems models were integrated into a baseline aircraft performance model, which was used to dynamically simulate the tank thermal behaviour during representative missions. The initial results indicate that switching to more electric environmental control and ice-protection systems likely have negligible thermal impact on the bulk fuel temperature. However, some benefits may be obtained regarding safety and certification, but this requires further study.

Introduction

Thermal management in aircraft is becoming an increasingly important topic. There are several reasons for this, many relating to new and higher localised heat loads associated with advances in propulsion and the electrification of subsystems[1] (i.e. the rise of the 'more electric aircraft'). Simultaneously, there is also a general decline in the availability of heat sinks. For example, the increase in the use of composite airframe skins, which have higher thermal resistance than Aluminium alloys, weakens the prospects of using the external atmospheric air for cooling purposes. Furthermore, additional increases in engine bypass ratios, (i.e. higher ratios of air mass flow through the bypass duct to engine core mass flow), are likely to further exacerbate this heat management problem. This is because increasing the bypass ratio leads to a reduction in engine core compartment ventilation (due to lower fan pressure ratios); additional heat sources arising from, for example, the incorporation of a fan power gearbox; as well as the need for thinner, "slimline" nacelles, which leave less room for heat dissipating equipment, such as heat exchangers, amongst many others[2].

The purpose of the work presented in this paper was to investigate the thermal effects of more electric systems on one of the most important heat sinks on civil transport aircraft – the fuel. This was necessary to understand how the ability of the fuel to act as a heat sink, especially in cooling down hot engine oil associated with higher bypass ratio engines, would be influenced. The work forms part of a larger multidisciplinary effort, the 'UHBR Thermals' Programme (Ultra-High Bypass Ratio). This Innovate UK and Meggitt PLC funded research programme investigates engine and airframe heat exchange concepts for future UHBR geared turbofan engines and quantifies their benefit on the system and aircraft level[3].

In particular, it was hypothesised that the electrification of the environmental control system (ECS) and ice protection system (IPS) would lead to reduced thermal loads on the fuel tank. This may enable the fuel to accept more heat from the engine, by means of several approaches, such as recirculation. It was therefore required to model the thermal behaviour of the fuel tank, the ECS and IPS (in both their conventional and more electric forms) in an integrated manner, along with the overall performance of the aircraft on representative missions. This paper reports on the modelling and simulation approach, the results obtained, and the possible implications of these results.

Background

Fuel as a heat sink

Fuel is often employed as one of the main heat sinks in both civil and military aircraft[1]. Heat generated by several systems (such as by the engine and hydraulic systems) is usually rejected to the fuel by means of heat exchangers that are situated either directly inside the tanks, or along the path the fuel takes outside the tanks on its way to the engine combustion chamber[1]. In some aircraft, the fuel is sometimes recirculated back to the fuel tank after collecting waste heat[4].

The fuel is well suited for this purpose as a cooling liquid, as its temperature can drop significantly during a mission. This is because the fuel tanks are usually integral to the wing structure and most of the barrier between the fuel and the cold atmosphere normally only consists of the structural skin. As the skin is traditionally manufactured from Aluminium alloys of high thermal conductivity, the fuel cools rapidly as the aircraft climbs to higher altitudes where the outside air temperature is considerably lower. However, the increase in the use of composites in airframe structures inevitably slows down

this cooling, as these materials have higher thermal resistances.

On large civil airliners, there is often also a centre fuel tank, which is formed as a structural continuation of the wing box inside the fuselage. It normally has a compartment directly underneath it, which houses components from the air conditioning system. This tank is therefore more isolated from the atmosphere, which leads to important additional thermal considerations.

Due to the large fuel temperature drops during a flight, rejecting heat to it has a twofold advantage – along with providing a means of cooling for heat generating systems, it also enables the temperature of the fuel to be raised to an acceptable level before entering the combustion chamber. The fuel cannot be allowed to become too cold, as it becomes difficult to pump below certain temperatures[5]. Higher fuel temperatures in the combustion chamber generally also have a beneficial effect on engine fuel consumption.

However, there are conditions when rejecting heat to the fuel could be dangerous. This could happen when the fuel in the tank is already at a high temperature, such as can occur when the aircraft remained on the ground for a sizable length of time in very hot conditions before taking off. In such cases, the fuel temperature becomes close to the lower flammability limit causing an increased risk of an explosion if an ignition source is present[1]. An infamous accident, that of Trans World Airlines (TWA) flight 800[6], serves as a tragic example. In that accident, a hot air-fuel mixture in the centre fuel tank contributed to an explosion that occurred shortly after take-off. The hot mixture was caused by a combination of the hot weather experienced on that day, a delay in departure (which resulted in more time for the fuel to be heated), and the running of the air conditioning packs that lie directly underneath the centre tank. Because of that accident, it is now required that heat transfer to the fuel tanks is limited and modern aircraft usually have nitrogen inerting systems to prevent ignition of the fuel vapours.

Therefore, although fuel is a convenient heat sink, it is important to manage the heat transferred to it to prevent it from becoming either too hot or too cold. Any change in systems architecture that could affect the fuel must be studied to understand the potential thermal implications involved. A switch to a more electric ECS and IPS constitutes exactly such a situation. The relevant aspects of behaviour of these systems as heat sources (for both conventional and more electric cases) are discussed briefly in the following section.

Airframe systems as fuel heat sources

Although many systems could be cooled down using fuel as a heat sink, only systems that generate substantial heat near the fuel tanks are considered here. These are the ECS, IPS, hydraulic equipment, and flight control actuators. For this paper, only the effects of the ECS and IPS are considered.

Conventional ECS and IPS architectures are typically powered by hot bleed air that is removed from the compressor stages of the engine. The associated ducting is usually close to the wing fuel tank front spar and heat is therefore transferred from the ducting to the fuel. Although often well insulated, some authors model the bleed air duct surface temperature to up to 75ºC[7].

A common placement of the air conditioning packs is to have them directly underneath the centre fuel tank. They can become substantially hot, with surface temperatures on the units of up to 176°C[6]. This heats up the compartment in which the packs are located by convection and this heat eventually transfers to the fuel.

More electric versions of the ECS and IPS eliminate the bleed air ducting as a heat source. The more electric ECS uses ram air, which is compressed by low-pressure air conditioning packs. They usually operate at lower temperatures than their bleed counterparts. For example, the more electric ECS compressors on the Boeing 787 deliver air at 90°C, compared with the 180°C associated with typical conventional bleed systems[8]. The more electric wing ice protection eliminates the pneumatic ‘piccolo’ tubes in the slats in favour of electric blankets that are attached directly to the interior of the leading-edge surface of the wing. These blankets are more energy-efficient and eliminate the circulating hot air associated with the pneumatic IPS as a heat source[9].

Wing and fuel tank thermal modelling approaches

Most past fuel tank thermal modelling work has taken the 1-D transient method for bulk fuel temperature estimation[10–12]. The setup for various tank geometries is simple and a swift computational solution can be obtained for even multi hour flight mission profiles. In the literature on military aircraft, combined fuel and system thermal modelling approaches have also been conducted (see for example McCarthy et al.[13] and Wolff[14]). However, for civil transport aircraft, such integrated research is less common, particularly for future engine configurations and airframe systems, pointing towards a need for further study. In particular, comparisons of conventional and more electric systems and their effect on the fuel as a heat sink, specifically for use in combination with higher bypass ratio engines, are required.

Modelling approach

The modelling and simulation framework serves the purpose of capturing the effects of the different systems on the fuel temperature over the entire duration of a mission. For this purpose, an integrated dynamic airframe, propulsion, and thermal management simulation framework, is currently being developed at Cranfield University, in partnership with Meggitt PLC.

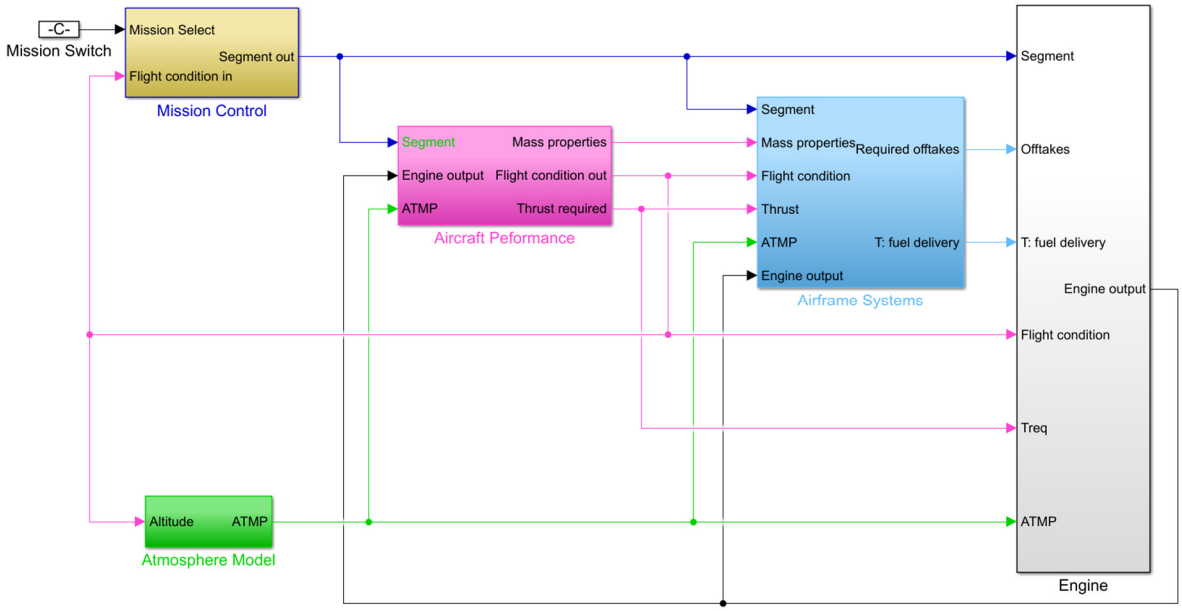

Figure 1: Top-level Simulink diagram of the simulation framework.

The objective was to establish a framework in which integrated thermal management concepts for both powerplants and airframes of civil transport aircraft can be modelled and dynamically simulated, as well as to analyse the overall effects at aircraft level. The framework is being developed in MATLAB® Simulink®. A baseline aircraft, representative of the Airbus A320, was selected for the work described in the paper.

Framework overview

The Simulink block diagram of the framework is provided in Figure 1, with five top-level blocks of 'Mission Control', 'Atmosphere', 'Aircraft Performance', 'Airframe Systems', and 'Engine blocks' shown. It enables the user to make variations in mission profile and parameters via the mission control block.

Atmospheric conditions are calculated in the Atmosphere Model block, which was developed based on the descriptions in MIL-STD-210[15].

The mission segment, atmospheric, and engine output (primarily fuel burn) information is used in the Aircraft Performance block to update flight conditions (climb/descent rates, speed and altitude) and calculate the thrust required from the engines.

The Airframe Systems block houses all the main aircraft systems, excluding propulsion systems. Along with simulating the thermal behaviour of the airframe and its systems, this block also calculates the secondary power engine-offtakes required by the systems.

The engine block contains detailed propulsion and engine thermal management system models. The engine model itself was created in Cranfield University's Turbomatch gas turbine modelling software[16]. This engine model is representative of a high bypass ratio (15 :1) engine with 25,000 lb thrust.

Fuel tank thermal model

The fuel tank thermal modelling philosophy is based on a 1-D transient heat transfer approach, with temperature varying heat transfer coefficients and fluid characteristics. The model contains a number of temperature nodes for structural components, fluid volumes and external atmospheric conditions. For the fuel system, such nodes represent the bulk fuel and ullage volumes and the bulk structural members, as shown in Figure 2.

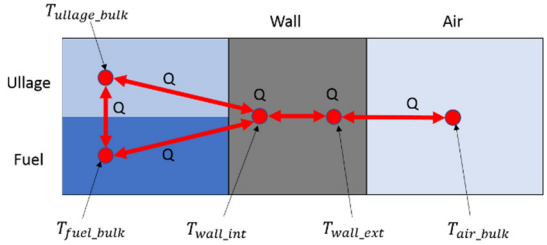

Figure 2: Tank thermal model temperature nodes and heat flows.

The node network is solved for its unknowns by equating the heat flow balance at each node with the change in its total heat capacity[17]. This is completed for all unknown node temperatures, resulting in a set of temperature-time derivatives, which are solved numerically. The initial conditions of all node temperatures are set in reference to the atmospheric conditions at the start of the mission and the refuel temperatures.

The tank simplification approach chosen for this work is visualized in Figure 3. Each tank is represented by two rectangular sections, aligned with the body-axis of the aircraft and separated along the span direction of the aircraft. These sections can be moved within the z-x plane to define tanks with dihedral and sweep.

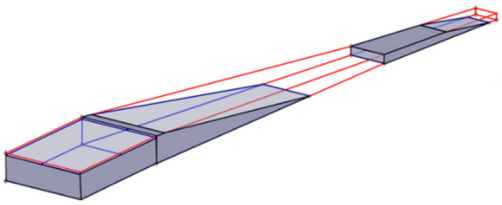

Figure 3: Tank geometry simplification.

After definition of the individual tank geometries, which make up the overall fuel storage possibilities on the aircraft, the geometry model can provide volume, area and reference fill state relationships for each individual tank, or the aircraft as a whole.

At each simulation timestep, convection heat transfer coefficients are calculated between the fluid (i.e. fuel, ullage, or air) and structural nodes. These are calculated with empirical equations obtained from Çengel[18] for vertical natural, horizontal natural, laminar, or turbulent convection, or forced convection with aerodynamic heating. To calculate the relevant Nusselt numbers, it was assumed that the fuel velocity in the tanks is about 1 m/s. This led to low Reynolds numbers which corresponded to laminar flow. For internal air and ullage, natural convection was assumed and for surfaces exposed to the external air, the true airspeed was used to calculate heat transfer coefficients. The convection heat transfer rate between a structural wall, i, and the fluid in contact with it is then calculated as follows:

$$\dot{Q}_{conv,i} = hA_{s,i}\Delta T \qquad (1)$$

In Equation 1, $\Delta T = T_{wall} - T_{bulk}$ is the difference in temperature between the structural and bulk fluid nodes, $A_{s,i}$ is the surface area of tank wall i, and h is the convection heat transfer coefficient. The convention is that $\dot{Q}_{conv,i}$ is positive if it the heat flows from the wall to the fluid.

Conduction through structural wall i for a given wall is calculated as follows:

$$\dot{Q}_{cond,i} = \frac{kA_{s,i}\Delta T}{t_{wall,i}} \qquad (2)$$

In this case, $\Delta T = T_{int} - T_{ext}$ is the difference in temperature between the interior and exterior of the wall, k is the thermal conductivity of the wall material, and $t_{wall,i}$ is the wall thickness. As can be seen, in this case, $\dot{Q}_{cond,i}$ is positive if the heat is transferred from the interior to the exterior of the wall.

The temperature of the bulk fluid can then be updated as follows (using the Euler method):

$$T_{bulk,n} - T_{bulk,n-1} = \frac{\left(\dot{Q}_{f,u} + \sum_{i=1}^{6}\dot{Q}_{conv,i}\right)}{C_{p,bulk}\rho_{bulk}V_{bulk}}\Delta t_{sim} \qquad (3)$$

In Equation 3, $T_{bulk,n}$ and $T_{bulk,n-1}$ are the temperatures at the current and previous timesteps; $\dot{Q}_{f,u}$ is the heat transfer rate between the fuel and ullage; the sum in the numerator represents the convection heat transfer at the six tank boundaries; and $C_{p,bulk}$, ρ_{bulk}, and V_{bulk} are the bulk fluid specific heat, density, and volume, respectively. The simulation timestep duration is given by Δt_{sim}.

Similarly, the temperature of the interior surfaces of tank wall i is updated as follows:

$$T_{i_{int},n} - T_{i_{int},n-1} = \frac{-\dot{Q}_{conv_{fuel},i} - \dot{Q}_{conv_{ullage},i} - \dot{Q}_{cond,i}}{C_{p,i}\rho_i V_i}\Delta t_{sim} \qquad (4)$$

Here, $\dot{Q}_{conv_{fuel},i}$ and $\dot{Q}_{conv_{ullage},i}$ are the convection heat transfer rates between the tank wall and the fuel and ullage, respectively. $C_{p,i}$, ρ_i, and V_i are the tank material specific heat, material density, and half of the volume occupied by the tank wall, respectively.

On the other hand, the exterior temperature of wall i is updated with the following equation:

$$T_{i_{ext},n} - T_{i_{ext},n-1} = \frac{\dot{Q}_{conv_{ext},i} + \dot{Q}_{conv_{aero},i} + \dot{Q}_{cond,i}}{C_{p,i}\rho_i V_i}\Delta t_{sim} \qquad (5)$$

In this case, $\dot{Q}_{conv_{ext},i}$ is the heat transfer rate between the surface and ambient air in ventilated compartments, such as in the fixed leading and trailing edges. $\dot{Q}_{conv_{aero},i}$ represents the heat transfer between the surface and the fast-moving ambient air (i.e. the top and bottom skins of the wing). Note that $\dot{Q}_{conv_{ext},i}$ and $\dot{Q}_{conv_{aero},i}$ would be zero if there is no contact between the wall and ambient air, for example, when the wall is between two fuel tanks.

Finally, the tank fill levels are updated based on the mass of fuel burned during the timestep and the feed temperature is assigned the bulk temperature of the fuel in the appropriate tank. This is controlled by the fuel burn sequence of the given aircraft and incorporated into the simulation. For the A320, the centre tank is emptied first (as is usual practice for most aircraft), followed by the inboard tank. When the inboard tank level drops below a certain point, fuel is transferred from the outboard tank. The fuel feed temperature is therefore the bulk fuel temperature of the centre tank, until it empties, then that of the inboard tank, and finally the average temperature of the mixture of inboard and outboard tank bulk fuel.

Fuel tank thermal model validation

The fuel tank thermal model was validated using data obtained for fuel temperatures in the inboard and outboard tanks across a representative flight for the Airbus A310. To perform the validation, the temperatures predicted by the model for the fuel in the inboard and outboard tanks were compared with the

published data[19]. It was found that the model produced similar trends as in the published data, but that heat transfer takes place at a slower rate. This was attributed to the possibility that the heat transfer between the tank walls and bulk fluids in the tank takes place by combined laminar and turbulent convection, rather than pure laminar convection, as originally assumed. Subsequently, the applicable heat transfer coefficients were increased manually, until a better fit was obtained.

It was subsequently found that, if the heat transfer coefficients were increased by a factor of 1.5 and 1.8 for the inboard and outboard tanks, respectively, an average temperature difference between model and published temperature data of less than 2ºC was obtained. Maximum errors were still high, however (up to 8.6ºC). These errors occurred during the ascent and descent phases, where it is expected that fuel sloshing and ventilation of the tanks with atmospheric air, phenomena that were not modelled, would have considerable influence.

Considering the simplicity of the model, these errors were deemed acceptable for the study in this paper. This is because the model would at least be able to provide ordinal comparisons for different thermal management architectures.

Systems component thermal models

To model the system components, a simple extension to the 1-D node approach described for the fuel tank thermal model was followed. This involved representing the system components as additional temperature/heat generation nodes. The resulting geometry and node-networks are illustrated in Figure 4 (planform view and side view of the centre tank) and Figure 5 (side view of a section of the wing).

In Figure 4, in addition to the fuel tanks, three more thermal compartments are shown (bounded by the dashed black lines). These include two fixed leading-edge compartments (four in total when the right wing is included) – one inboard of the engine and one outboard. These are located just behind the slats and directly in front of the front spars. The other additional compartment is the bay which houses the ECS pack. This compartment extends from the front to directly beneath the centre fuel tank. As with the fuel tank surfaces, the structural walls bounding these additional compartments each have internal and external wall temperature nodes, to capture their thermal mass and temperature response.

The bleed air duct is represented by the red lines in Figure 4. Note that the bleed air duct outboard of the engine (represented by the dashed red line) only transports bleed air when the IPS is activated. The thermal nodes for the bleed air ducts are represented by the red dots. The heat transfer from the ducts to the bulk air in the compartments were modelled as natural convection over cylinders (see Çengel[18]). The geometries of the ducts were obtained from the Airbus A319 maintenance manual[20].

The dashed yellow line represents the piccolo tube. As with the bleed air duct outboard of the engine, bleed air only flows through this duct when the IPS is activated. The yellow dot represents the thermal nodes associated

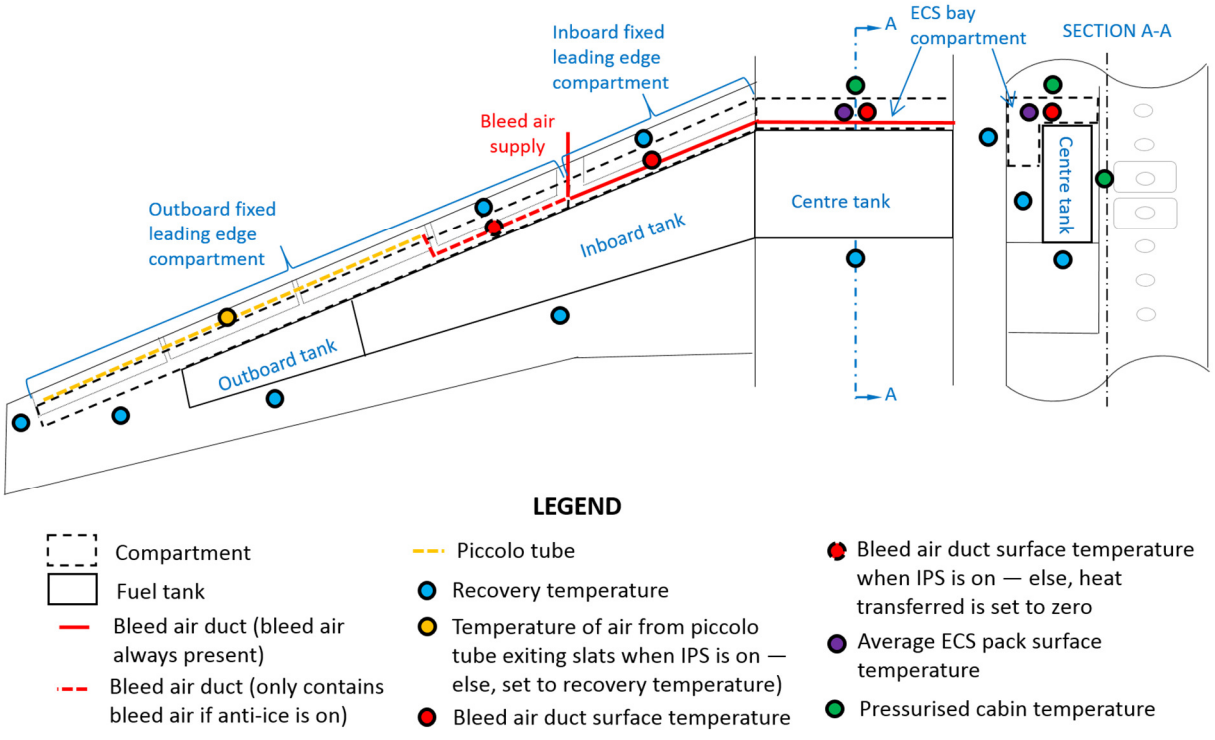

Figure 4: ECS and IPS thermal node network (planform view).

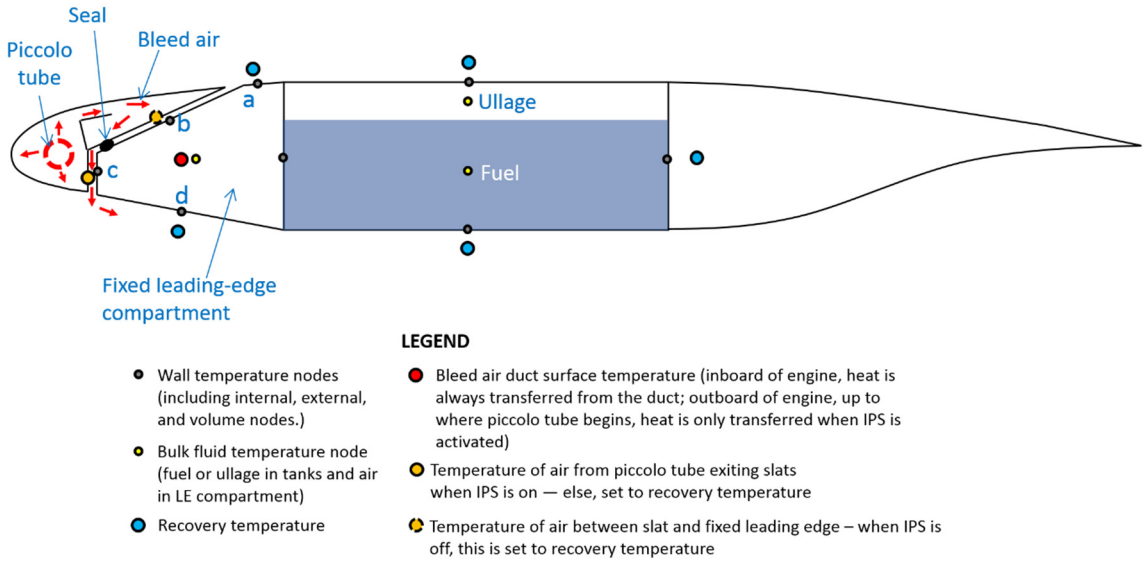

Figure 5: Wing thermal node network (sectioned side view).

with the piccolo tube. Two were modelled – one for the hot air exiting the slat (flowing over surface c in Figure 5) and one for the air trapped in between the slat and the leading edge (surface b). The geometry of the fixed leading edge was estimated and simplified from Scholz[21]. For surface b, the heat transfer was modelled as natural convection over an inclined plate[18] and as forced convection over a flat plate[18] for surface c. The mass flow rate per unit span was set at 0.1 kg/s.m (an assumption, based on about 0.05 kg/s.m used for business jets in Domingos, Papadakis, and Zamora[22] – i.e., it was assumed that the leading edge of the A320 would be about twice as thick on average as the business jet's). From this mass flow, an average velocity of the air flowing over surface c was estimated to be about 9.2 m/s, assuming the gap between the slat and the surface is about 1.2 cm on average.

The thermal node associated with the two ECS packs is represented by the purple dots in Figure 4. The heat transfer from the ECS pack to the bulk air in the ECS bay compartment was modelled as natural convection over a flat plate. Representative geometry for the Airbus A320 ECS pack and the ECS bay were estimated from the Airbus A319 maintenance manual[20] (the A319 and A320 geometries are assumed to be the same).

In Figure 4 and Figure 5, the boundary conditions are represented by blue dots (external flow temperatures, i.e. recovery temperature) and green dots (air temperature in pressurised compartments – set to the cabin temperature).

For simulating the more electric case, the bleed air and piccolo ducts are removed (i.e. the heat contribution from these are set to zero). It was assumed that the effect of heat generated on surfaces b and c (Figure 5) by electrical anti-ice heating matts would be negligible.

Simulation setup

The simulation was set up for a mission representative of the design mission of the Airbus A320. The salient mission parameters are provided in Table 1. Note that, as it was only required to perform an ordinal comparison between the conventional and more-electric systems, only ISA conditions were applied.

Table 1: Salient mission parameters.

Mission Parameter	*Value*
Cruise altitude	10 000 m
Cruise Mach no.	0.78
Distance flown	3 550 km
Flight duration	4 hrs 40 min
Take-off weight	73 500 kg
Payload	14 250 kg (150 pax)
Fuel load	17 000 kg
Simulation time step	5 s

Because of the considerable uncertainty in the models and the actual component temperatures, a factorial design of experiments was set up. In this setup, the relevant component temperatures were varied as listed in Table 2. These temperature ranges were assumed but it is unlikely that actual values would fall outside of them. Note that only appropriate combinations were run. A baseline case was set to be one where no heat transfer due to these components was considered (i.e. all 'off').

Table 2: Design of experiments setup.

Temperature	*Values [°C]*
Bleed duct surface (T_{bld})	{off, 25,50,75}
Air over surface b ($T_{air,b}$)	{off, 0, 20, 40}
Air over surface c ($T_{air,c}$)	{off, 0, 50,100}
ECS pack surface (T_{ECS})	{off, 50,75,100,125}

In the above table, the more-electric cases would correspond to runs where the bleed air heat transfer is disabled (i.e. selected to be 'off').

As the fuel tank bulk temperatures from the simulation directly link to the fuel feed temperature that the engines receive, an inference regarding the engine's cooling capability can be made. Specifically, the fuel usually passes an engine oil-fuel heat exchanger, in which waste heat from engine components is rejected via the oil to the fuel. Therefore, for each of the runs, the time history of the fuel feed temperature was logged for the whole duration of the mission. The maximum heat that could be transferred to the fuel (by means of the engine fuel-oil heat exchanger) over the whole mission could then be calculated as follows:

$$Q_{mission} = \int_0^{t_{tot}} \dot{Q}(t)\, dt \qquad (6)$$

where t_{tot} is the total duration of the mission and

$$\dot{Q}(t) = \dot{m}(t) c_{p,fuel} (408 - T_{fuel}(t)) \qquad (7)$$

In equation 2, $\dot{m}(t)$ is the mass flow rate of the fuel feed, $T_{fuel}(t)$ is the temperature of the fuel at time t, $c_{p,fuel}$ is the specific heat of Jet A1 fuel (calculated at the average of 408 K and $T_{fuel}(t)$, using information from the Handbook of Aviation Fuel Properties[23]). The value of 408 K is the assumed maximum temperature that the fuel can be raised to before entering the combustion chamber.

Results and discussion

Effects of bleed air exiting slats

Table 3 shows the percentage difference in total heat that can be transferred to the fuel over a full mission for different cases of air temperatures over surfaces b and c (see Figure 5). The baseline case is for when the temperatures are set to the recovery temperature (i.e. when there is no effect modelled for the air temperature over surfaces a and c). For the results in this table, the effects of other systems were disabled. As mention before, the increased temperatures over surfaces b and c only apply when the wing anti-ice is activated. When the anti-ice is off, these temperatures are set equal to the recovery temperature.

Table 3: Differences in heat transferable to fuel for different cases of air temperature exiting slats.

$T_{air,b}$ [°C]	$T_{air,c}$ [°C]	$\Delta Q/Q_{EECS} \times 100$ [%][a]
0	0	-9.5×10^{-8}
20	50	-2.2×10^{-6}
40	100	-4.4×10^{-6}

Note: (a) Baseline case: $T_{air,b} = T_{air,c} = T_{rec}$.

As can be seen from the table, the effects of bleed air exiting the slat and impinging on the fixed leading edge was determined to have a negligible effect on the heat transferable to the fuel. This can be attributed to the short durations of time during which the wing anti-ice is activated; the relatively small areas exposed to the hot air; and the relatively large mass of air in the fixed leading edge; which, together, amounts to a large thermal resistance. Because of this, the anti-ice was excluded from the rest of the study.

Effects of bleed air duct surface temperature

Figure 6 shows the estimated effects that different bleed air duct surface temperatures have on the bulk fuel temperatures, when other contributing system heat sources (i.e. the ECS pack and bleed air exiting the slats) are disabled. The temperatures shown are for the centre tank, inboard tank, and outboard tank bulk fuel temperatures, for when the bleed air contribution is disabled (i.e. $Q_{bld} = 0W$), along with cases where the duct surface temperature is at 25°C, 50°C, and 75°C.

As can be seen in the figure, the effects of the bleed air duct temperature on the outboard tank is estimated to be negligible. This is because there is no bleed air duct in the fixed leading edge directly in front of the outboard tank. In fact, the only significant heat contribution comes from the bleed duct in front of the inboard tank, which only houses bleed air during the short phases in the flight when the anti-ice is activated.

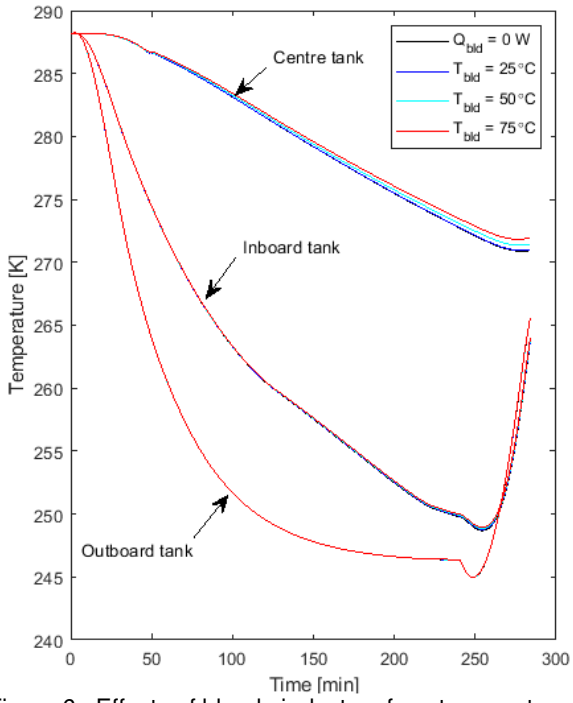

Figure 6 : Effects of bleed air duct surface temperatures on bulk fuel temperatures.

There is indeed a noticeable effect on the inboard tank. However, this is still very small (a final temperature difference of about 0.3°C for the case when $T_{bld} = 75$°C) and is considered here to be negligible. The small effect can be attributed to only a small area of the tank (i.e. the front spar, inboard of the engine) being exposed to a compartment in which the bleed air duct (through which bleed air continuously flows) is housed.

The effects on the centre tank are only slightly more significant. End-of-flight fuel temperature differences of about 0.6°C and 1.1°C can be seen for the cases when $T_{bld} = 50$°C and $T_{bld} = 75$°C, respectively. These higher

temperature differences are attributed to the centre tank being exposed to the air in the ECS compartment, which is constantly being heated by the hot bleed air duct.
The effects on the bulk ullage temperatures in the three tanks are not shown, but are even less pronounced than on the bulk fuel temperatures. A maximum final temperature difference of only $0.6℃$ was found between the 'off' and $T_{bld} = 75℃$ cases.

Effects of ECS pack surface temperatures
The effects of different ECS pack surface temperatures on the centre fuel tank ullage and fuel bulk temperatures are shown in Figure 8. The plot shows the bulk temperatures for four cases: no ECS contribution ($Q_{ECS} = 0W$), and pack surfaces temperatures of $50℃$, $75℃$, $100℃$, and $125℃$. Note that the effects on the inboard and outboard tank were found to be negligible and are not shown here.

As can be seen in the figure, the effects due to the ECS pack are somewhat more significant than those related to the bleed air duct. In the most severe case (with the pack surface at $125℃$), the final temperature differences in the bulk fuel was predicted to be up to $4.1℃$, whereas that of the ullage was predicted to be up to $2℃$.

These results indicate that, if the ECS pack were to operate at considerably lower temperatures through electrification, a considerable difference in fuel temperature in the centre tank might be obtained. This may have benefits regarding safety and certification, but a more in-depth investigation, especially involving extreme atmospheric conditions, will have to be conducted to determine what these might actually entail.

It is worth mentioning that the centre tank is usually inerted and the aforementioned temperature differences would likely be too small to permit a removal of the inerting system.

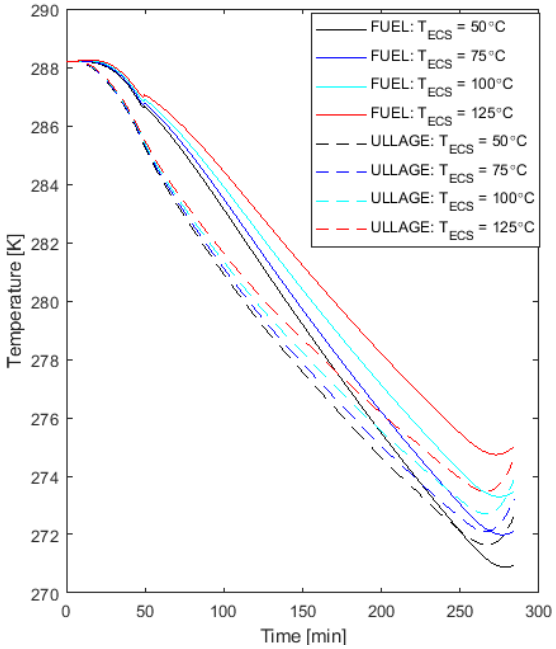

Figure 8: Effect of average ECS pack surface temperatures on fuel and ullage bulk temperatures in the centre tank.

Effects on heat transferable to fuel at engine fuel-oil heat exchanger
The effects of the combined ECS pack and bleed air duct surface temperatures on the fuel feed temperature are shown in Figure 7. As can be seen, the largest temperature differences occur between about 48 and 62

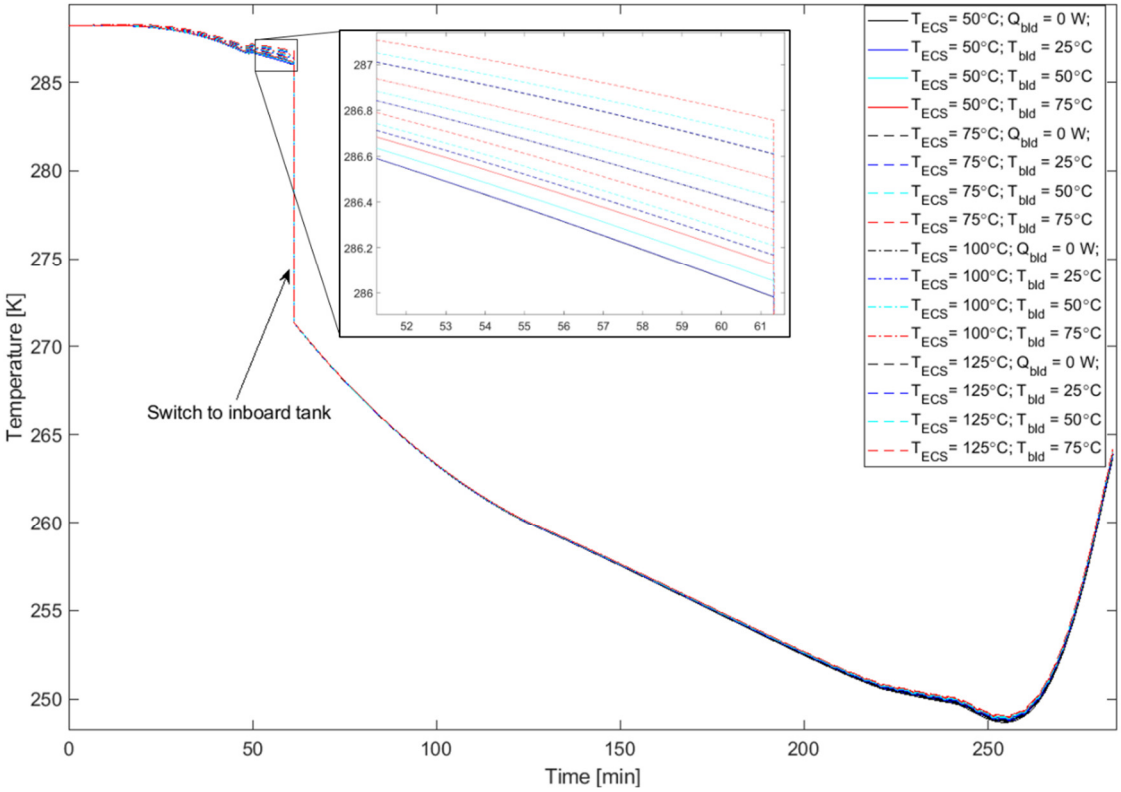

Figure 7: Fuel feed temperature histories for different combinations of ECS and bleed duct surface temperatures.

minutes into the flight. This is just before the centre tank empties and the feed switches to the inboard tank. After the feed switches to the inboard tank, the differences in temperature are miniscule, but increases slightly as the flight continues.

The fuel feed temperature histories were used to determine the amount of heat that can be rejected to the fuel at the engine fuel-oil heat exchanger over the whole mission, for different combinations of ECS pack and bleed air duct surface temperatures (using Equation 2). The results are shown in Figure 9. As can be seen, the differences in transferable heat, ranges in the megajoules. In the case that the operating temperature of the ECS pack remains unchanged after electrification, additional heat of about 3.4 MJ could be transferred, compared with a bleed case where the bleed air duct surface temperature was 75°C.

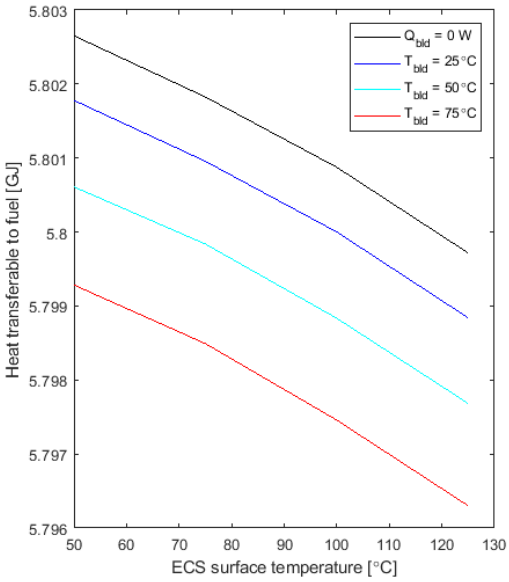

Figure 9: Heat transferable to fuel for different combinations of ECS and bleed duct surface temperatures.

Similarly, if the bleed duct temperature effects are neglected, a difference in heat transferable of about 3 MJ can obtained between the case where the ECS pack surface temperature is 50°C and that where it is 125°C.

Discussion

The studies presented in this section show that any benefit regarding the amount of heat that could be transferred to the fuel when switching to more electric systems is likely to be negligible. Even a component that has a constant heat loss rate of only 1 kW over the 283-min mission will contribute about 17 MJ in total heat. If such a load would be added, it will totally consume the 3 MJ that could possibly be gained when switching to more electric systems. The heat loads on future UHBR engines ratios are expected to be more than double current heat loads (largely due to the introduction of the fan power gearbox). These losses will be in the 100s of kilowatts, which dwarfs this example 1kW load.

Furthermore, the additional heat produced by the electrical generators to power the more electric systems need to be accounted for as well, as this heat will also have to be removed. Even with more efficient generators, the additional heat produced by them when powering the more electric systems would likely far exceed the values that can be gained from removing the bleed air and operating the ECS at lower temperatures.

In terms of safety and certification, the effects on the centre tank bulk fuel and ullage temperatures are not entirely trivial. At the very least, a slight increase in safety margin might be obtained when removing the bleed air and if the ECS pack could be operated at a lower temperature after electrification.

Finally, as the results presented in this paper are only for bulk fuel and ullage temperatures, resulting from a 1-D thermal model, there is no indication regarding what local effects may be present on the fuel and ullage temperatures. These may be significant and require further study.

Conclusions

The hypothesis for the study presented in this paper was that the electrification of the environmental control system (ECS) and ice protection system (IPS) would lead to reduced thermal loads on the fuel tank, which would enable the fuel to accept more heat from the engine. It was expected that this may be beneficial when considering the much larger thermal loads expected for future ultra-high bypass turbofan engines. The results, obtained from executing the combined flight performance and 1D thermal model developed for the wing for several different cases over a representative mission, indicate that the benefits would likely be negligible. Specifically, the additional heat loads associated with the larger bypass ratio engines are expected to significantly exceed the extra heat that could be rejected to the fuel if the bleed air duct were to be removed and if the more electric ECS were to be operated at lower temperatures. However, some advantages may be gained in terms of safety and certification, as the differences in centre tank fuel and ullage temperatures for the different cases were found to be nontrivial.

With no substantial benefits in terms of being able to reject additional waste heat to the fuel when switching to more electric architectures, the need for novel thermal management systems for UHBR engines is further underpinned. Future work would therefore focus on employing the simulation framework developed for this research to study different possible solutions to this problem.

References

1. Ahlers, M. F. Aircraft Thermal Management. in *Encyclopedia of Aerospace Engineering* (Wiley Online Library, 2010). doi:10.1002/9780470686652.eae046
2. Verseux, O. & Sommerer, Y. New challenges for engine nacelle compartments pressure and thermal loads management with aircraft engine evolution. *29th Congr. Int. Counc. Aeronaut. Sci. ICAS 2014* (2014).
3. Aerospace Technology Institute. UHBR Thermals project. *Press Release* (2017). Available at: https://www.ati.org.uk/2017/11/ati-fundingenables-%0Ameggitt-research-thermal-systems-technology/.
4. Langton, R., Clark, C., Hewitt, M. & Richards, L. *Aircraft fuel systems*. **24,** (John Wiley & Sons, 2009).
5. Kornstaedt, L. Low fuel temperatures. *Airbus FAST Magazine* 5–11 (2005).
6. National Transportation Safety Board. In-flight breakup over the Atlantic Ocean, Trans World Airlines Flight 800, Boeing 747–131, N93119, near East Moriches, New York, July 17, 1996. (2000).
7. Zilio, C. *et al.* CFD analysis of aircraft fuel tanks thermal behaviour. in *Journal of Physics: Conference Series* **923,** 12027 (IOP Publishing, 2017).
8. Martinez, I. Aircraft environmental control (lecture notes). (2014).
9. Sinnett, M. 787 no-bleed systems: saving fuel and enhancing operational efficiencies. *Aero Q.* **18,** 6–11 (2007).
10. Guan, T. Fuel System Water/Ice Management Using OBIGGS. (Cranfield University, 2014).
11. Terada, Y., Lawson, C. P. & Shahneh, A. Z. Analytical investigation into the effects of nitrogen enriched air bubbles to improve aircraft fuel system water management. *Proc. Inst. Mech. Eng. Part G J. Aerosp. Eng.* 0954410017742422 (2017).
12. Kang, Z., LIU, Z., REN, G. & LV, Y. *Fuel Tank Modeling and Fuel Temperature Simulation of an Aircraft in Steady-State and Transient-State Methods*. (2015). doi:10.13140/RG.2.1.3000.9681
13. McCarthy, K. *et al. Dynamic Thermal Management System Modeling of a More Electric Aircraft*. (SAE Technical Paper 2008-01-2886, 2008).
14. Wolff, M. *Aerothermal Design of an Engine / Vehicle Thermal Management System*. (2011). doi:10.14339/RTO-EN-AVT-195
15. MIL-STD-210C. Climatic information to determine design and test requirements for military systems and equipment. (1987).
16. Cranfield University. *The TURBOMATCH Scheme*. (1999).
17. Lienhard IV, J. H. & Lienhard V, J. H. *A Heat Transfer Textbook*. (Phlogiston Press, 2018).
18. Çengel, Y. A. *Heat and mass transfer*. (McGraw-Hill, 2006).
19. Judt, D. M., Lawson, C. P., van Heerden, A. S. J. & Bosak, D. Modelling of future engine and airframe integrated thermal systems concepts. in *SAE Aerospace systems and technology conference* (2018).
20. Airbus. Airbus A319: Aircraft Maintenance Manual. (2005).
21. Scholz, D. Aircraft Systems Lecture Notes. 9–15 (2007).
22. Domingos, R., Papadakis, M. & Zamora, A. Computational methodology for bleed air ice protection system parametric analysis. in *AIAA Atmospheric and Space Environments Conference* 7834 (2010).
23. Coordinating Research Council. *Handbook of aviation fuel properties*. (Society of Automotive Engineers, 1983).

Acknowledgments

This work was conducted under the Ultra High Bypass Ratio Aero Engine Thermal Systems (UHBR Thermals) Programme, funded by Meggitt PLC, as lead partner, and Innovate UK (grant No: 91855-263266).